Inorganic Chemistry

Article

pubs.acs.org/IC

# The Rhenium Tris(dithiolene) Electron Transfer Series: Calibrating Covalency

Stephen Sproules,*[†,‡] Thomas Weyhermüller,[†] Richard Goddard,[§] and Karl Wieghardt[†]

[†]Max-Planck-Institut für Bioanorganische Chemie, Stiftstrasse 34-36, D-45470 Mülheim an der Ruhr, Germany

[‡]EPSRC National UK EPR Facility and Service, Photon Science Institute, The University of Manchester, Oxford Road, Manchester M13 9PL, U.K.

[§]Max-Planck-Institut für Kohlenforschung, Kaiser-Wilhelm-Platz 1, D-45470 Mülheim an der Ruhr, Germany

Supporting Information

**ABSTRACT:** Four members of the rhenium tris(dithiolene) electron transfer series have been prepared, $[Re(S_2C_2R_2)_3]^z$ {R = Ph, $z$ = 1+ (**1**), 0 (**2**), 1− (**3**); R = CN, $z$ = 2− (**4**)}, with the anions in **3** and **4** structurally characterized. The intraligand C−S and C−C bond lengths for **3** vs **2** are indicative of ligand reduction concomitant with an overall distorted trigonal prismatic geometry (Θ = 26.3° cf. 3.8° in **2**). The distorted octahedral $ReS_6$ polyhedron in **4** (Θ = 38.3°) indicates reduction of the metal to a Re(IV) $d^3$ central ion. This series has been probed by sulfur K-edge X-ray absorption spectroscopy (XAS), and the electronic structures are unambiguously defined as follows: $[Re^V(L_3^{4-})]^{1+}$ ($S$ = 0) for the monocation in **1**; $[Re^V(L_3^{5-\bullet})]^0$ ($S$ = $^1/_2$) for neutral **2**; $[Re^V(L_3^{6-})]^{1-}$ ($S$ = 0) for the monoanion in **3**; and $[Re^{IV}(L_3^{6-})]^{2-}$ ($S$ = $^1/_2$) for the dianion in **4**. The sulfur 3p character in the frontier orbitals—the covalency—is estimated by two different approaches. Method A utilizes the radial dipole integral ($I_s$) derived from the S 1s → 4p transition, whereas method B, involves time-dependent density functional theoretical (TD-DFT) calculation of the pre-edge transitions and calibrated to the intensity in $[Re(pdt)_3]$ ($pdt^{2-}$ = 1,2-diphenyl-1,2-dithiolate). The two estimates are contrasted for the rhenium series and extended to the $[V(pdt)_3]^{0/1-}$, and $[Mo(mdt)_3]^{0/1-/2-}$ ($mdt^{2-}$ = 1,2-dimethyl-1,2-dithiolate) series, ultimately providing a refined description of the contested electronic structure of neutral molybdenum (and tungsten) tris(dithiolenes) compounds.

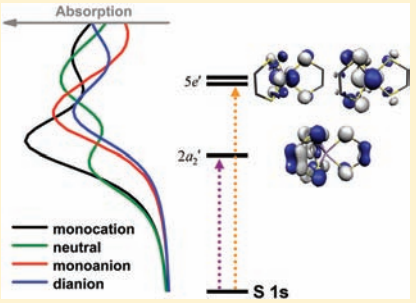


## INTRODUCTION

Trigonal prismatic geometry catapulted into coordination chemistry with the crystallographic characterization of $[Re(pdt)_3]$ (**2**; $pdt^{2-}$ = 1,2-diphenyl-1,2-dithiolate).[1] Prior to this moment, such a geometry was thought unattainable for a molecular six-coordinate complex because of the overwhelming repulsion between the closely spaced ligands.[2,3] It was recognized that an intrinsic electronic property of tris(dithiolene) complexes stabilized a trigonal prism over an octahedron and subsequent studies focused on elucidating the electronic structures of these complexes.[4−6]

Electrochemically, it has been established that $[Re(pdt)_3]$ (**2**) constitutes an electron transfer series where the neutral form can be reversibly transformed by one-electron transfer waves to the corresponding monocation, monoanion, and dianion: $[Re(pdt)_3]^z$ ($z$ = 1+, 0, 1−, 2−).[6,7] In the case of $[Re(mnt)_3]^{2-}$ ($mnt^{2-}$ = maleonitriledithiolate), the tri- and tetraanions are also electrochemically accessible.[8,9] From geometry optimization of the rhenium tris(dithiolene) series using density function theory (DFT) it was shown that traversing from monocation to trianion results in a twist about the $C_3$ axis to a distorted octahedral geometry for the more reduced members,[10] as measured by the trigonal twist angle, Θ (0° in a trigonal prism; 60° in an octahedron).[2] More interestingly, the optimized geometry of the monocationic member of the series yielded only a $D_{3h}$ symmetric structure. This was surprising because isoelectronic neutral molybdenum and tungsten complexes,[11] and the monoanionic vanadium species[12] all exhibit a sizable dithiolene fold − a distortion that lowers the point symmetry to $C_{3h}$.[13] This enables the frontier orbitals, specifically the highest occupied and lowest unoccupied molecular orbitals (HOMO and LUMO), to mix.[14] Therefore, the single structural distortion seen across this series presents an opportunity to probe the metal−ligand covalency in all tris(dithiolene) complexes because the trigonal twist ($D_{3h}$ → $D_3$) maintains an orthogonal HOMO and LUMO, unlike dithiolene folding ($D_{3h}$ → $C_{3h}$).

Sulfur K-edge X-ray absorption spectroscopy (XAS) is a proven method for directly probing metal−sulfur bonding in coordination compounds and enzymes.[15] The technique uses tunable synchrotron radiation around 2472 eV to drive an electric dipole allowed (s → p) excitation of the sulfur 1s core electron into the unoccupied 4p orbitals (edge feature). Additional features at lower energy known as pre-edge transitions arise from excitations to partially occupied or unoccupied metal d orbitals with contributions from sulfur 3p

**Received:** August 1, 2011
**Published:** November 10, 2011

   dx.doi.org/10.1021/ic2016534 | *Inorg. Chem.* 2011, 50, 12623−12631

orbitals. Their intensity reflects the sulfur 3p character of the acceptor orbital and therefore diagnostic of covalency.

We have chemically one-electron oxidized $[Re(pdt)_3]$ (**2**) to produce the first ever monocationic tris(dithiolene) compound, $[Re(pdt)_3](SbCl_6)$ (**1**). Additionally, the mono- and dianionic species, $[PPh_4][Re(pdt)_3]$ (**3**) and $[PPh_4]_2[Re(mnt)_3]$ (**4**) have been isolated and structurally characterized (Chart 1). The latter is the first structurally characterized dianionic tris(dithiolene) complex of rhenium. Subjecting these four compounds to S K-edge XAS, we have contrasted two methods of estimating ground state covalency. The first was devised by Solomon and co-workers and utilizes the radial dipole integral of the S 1s → 3p transition,[15−18] whereas the other involves a simple time-dependent (TD) DFT approach[19−21] calibrated to a specific compound, in this case **2**. These methods of estimation have also been extended to the $[V(pdt)_3]^{0/1-}$,[12] and $[Mo(mdt)_3]^{0/1-/2-}$ ($mdt^{2-}$ = 1,2-dimethyl-1,2-dithiolate) series,[22] and present a means by which the sulfur contribution to bonding in any tris(dithiolene) complex can be evaluated. This afforded a more meaningful description of the contested electronic structure assignment of neutral molybdenum tris(dithiolenes).

**Chart 1. Ligands and Complexes**

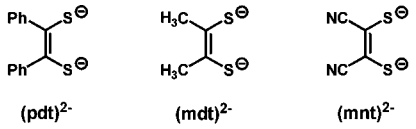


| | | |
|---|---|---|
| $[Re(pdt)_3](SbCl_6)$ | S = 0 | **1** |
| $[Re(pdt)_3]$ | S = 1/2 | **2** |
| $[PPh_4][Re(pdt)_3]$ | S = 0 | **3** |
| $[PPh_4]_2[Re(mnt)_3]$ | S = 1/2 | **4** |

## EXPERIMENTAL SECTION

**Synthesis of Complexes.** All air-sensitive materials were manipulated using standard Schlenk techniques or a glovebox. The complexes $[Re(pdt)_3]$ (**2**),[5] and $[PPh_4]_2[Re(mnt)_3]$ (**4**),[9] have been synthesized according to literature procedures.

**$[Re(pdt)_3][SbCl_6]$ (1).** Neutral **2** (100 mg; 0.11 mmol) dissolved in dichloromethane (10 mL) was treated with tris(4-bromophenyl)-ammoniumyl hexachloroantimonate ("Magic Blue"; 92 mg; 0.11 mmol) and stirred for 1 h at ambient temperature. The dark solution was filtered and the filtrate added to methanol (10 mL) to afford a dark green precipitate of **1**. This solid was collected by filtration, washed with methanol, then diethyl ether and dried under vacuum. Yield: 67 mg (49%).

Anal. Calcd for $C_{42}H_{30}S_6Cl_6SbRe$: C, 40.43; H, 2.42. Found: C, 41.02; H, 2.34.

**$[PPh_4][Re(pdt)_3]$ (3).** A tetrahydrofuran (THF; 10 mL) solution of **2** (100 mg; 0.11 mmol) was treated with *n*-BuLi (1.6 M in hexanes; 70 $\mu$L; 0.11 mmol) and stirred for 1 h. The solution was filtered into MeOH (10 mL) containing $PPh_4Br$ (48 mg; 0.114 mmol) affording **3** as a chocolate brown microcrystalline solid. This was collected by filtration, washed with methanol, and dried under vacuum. Yield: 110 mg (80%).

Anal. Calcd for $C_{66}H_{50}PS_6Re$: C, 63.28; H, 4.02. Found: C, 63.53; H, 4.07.

**X-ray Crystallographic Data Collection and Refinement of the Structures.** Single crystals of **3**·DMF and **3**·DMA were grown by diffusion of methanol into a saturated *N*,*N*′-dimethylformamide (DMF) or *N*,*N*′-dimethylamine (DMA) solution of the complex, whereas single crystals of **4** were obtained by slow diffusion of methanol into a saturated acetone solution of the complex. Suitable crystals were coated with perfluoropolyether, picked up with nylon loops and were immediately mounted in the nitrogen cold stream of the diffractometers. A Bruker-Nonius Kappa CCD diffractometer and graphite monochromated Mo−K$\alpha$ radiation ($\lambda$ = 0.71073 Å) from a Mo-target rotating-anode X-ray source was used for compounds **3**·DMF and **3**·DMA. Diffraction data of complex **4** were collected using a combination of $\omega$ and $\phi$ scans (10s/1° scan) on a Bruker-AXS Smart APEX-II diffractometer, located at the SCD beamline at the ANKA synchrotron facility, Karlsruhe, Germany. The radiation used was Si(111) monochromated radiation with a wavelength of 0.8 Å. Data were integrated with the program SAINT[23] and averaged using SADABS.[24] Final cell constants were obtained from least-squares fits

**Table 1. Crystallographic Data**

| | 3·DMF | 3·DMA | 4 |
|---|---|---|---|
| chem. formula | $C_{69}H_{57}NOPReS_6$ | $C_{70}H_{59}NOPReS_6$ | $C_{60}H_{40}N_6P_2ReS_6$ |
| Fw | 1325.69 | 1339.71 | 1285.48 |
| space group | $P2_1/n$, No. 14 | $P2_1/n$, No. 14 | *Pbcn*, No. 60 |
| *a*, Å | 14.2201(6) | 14.1730(10) | 20.032(8) |
| *b*, Å | 31.3790(9) | 31.364(3) | 15.316(6) |
| *c*, Å | 14.7466(6) | 14.7187(12) | 18.062(7) |
| $\beta$, deg | 116.663(3) | 116.539(4) | 90 |
| *V*, Å | 5880.4(4) | 5853.4(8) | 5542(4) |
| *Z* | 4 | 4 | 4 |
| *T*, K | 100(2) | 100(2) | 150(2) |
| $\rho$ calcd, g cm$^{-3}$ | 1.497 | 1.520 | 1.541 |
| refl. collected/$2\Theta_{max}$ | 149706/60.00 | 304224/65.00 | 197019/66.26 |
| unique refl./$I > 2\sigma(I)$ | 17126/15194 | 21162/19747 | 7220/6026 |
| No. of params/restr. | 816/169 | 745/47 | 339/0 |
| $\lambda$, Å /$\mu$(K$\alpha$), cm$^{-1}$ | 0.71073/23.52 | 0.71073/23.64 | 0.80/25.22 |
| R1[a]/goodness of fit[b] | 0.0337/1.047 | 0.0499/1.325 | 0.0363/1.224 |
| wR2[c] ($I > 2\sigma(I)$) | 0.0751 | 0.1094 | 0.0778 |
| residual density, e Å$^{-3}$ | +1.20/−0.92 | +2.63/−6.382 | +0.65/−1.07 |

[a]Observation criterion: $I > 2\sigma(I)$. R1 = $\sum||F_o| - |F_c||/\sum|F_o|$. [b]GoF = $\{\sum[w(F_o^2 - F_c^2)^2]/(n-p)\}^{1/2}$. [c]wR2 = $\{\sum[w(F_o^2 - F_c^2)^2]/\sum[w(F_o^2)^2]\}^{1/2}$ where $w = 1/\sigma^2(F_o^2) + (aP)^2 + bP$, $P = (F_o^2+2F_c^2)/3$.


dx.doi.org/10.1021/ic2016534 | Inorg. Chem. 2011, 50, 12623−12631

of several thousand strong reflections. Intensity data were corrected for absorption using intensities of redundant reflections with the program SADABS. The structures were readily solved by Patterson methods and subsequent difference Fourier techniques. The Siemens ShelXTL[25] software package was used for solution and artwork of the structures, and ShelXL97[26] was used for the refinement. All non-hydrogen atoms, except those of an ill-defined DMF molecule of solvation in **3**·DMF, were anisotropically refined and hydrogen atoms were placed at calculated positions and refined as riding atoms with isotropic displacement parameters. A diphenyldithiolene ligand (S41–C56) and a neighboring DMF molecule of solvation were found to be severely disordered in crystals of **3**·DMF. A split atom model comprising three different ligand and DMF orientations was refined giving an occupation ratio of about 0.63:0.22:0.15, respectively. SAME, EADP, and SADI restraints of ShelXL97 were used for the refinement. A similar situation was detected in isomorphous crystals of **3**·DMA. A phenyl group of the dithiolene ligand and an adjacent DMA molecule were treated using an analogous split model. Crystallographic data of the compounds are listed in Table 1.

**X-ray Absorption Spectroscopy.** All data were measured at the Stanford Synchrotron Radiation Lightsource (SSRL) under ring conditions of 3.0 GeV and 60–100 mA. S K-edge data were measured using the 56-pole wiggler beamline 6–2 and 20-pole wiggler beamline 4–3 in a high-magnetic field mode of 10 kG with a Ni-coated harmonic rejection mirror and a fully tuned Si(111) double-crystal monochromators. Details of the optimization of this setup for low-energy have been previously described.[27] All samples were measured at room temperature as fluorescence spectra using a Lytle detector. Samples were ground finely and dispersed as thinly as possible on Mylar tape to minimize the possibility of fluorescence saturation effects. Data represent 2–3 scan averages. All samples were monitored for photoreduction throughout the course of data collection. The energy was calibrated using the S K-edge spectrum of $Na_2S_2O_3·5H_2O$, run at intervals between sample scans. The maximum of the first pre-edge feature in the spectrum was fixed at 2472.02 eV. A step size of 0.08 eV was used over the edge region. Data were averaged, and a smooth background was removed from all spectra by fitting a polynomial to the pre-edge region and subtracting this polynomial from the entire spectrum. Normalization of the data was accomplished by fitting a flattened polynomial or straight line to the post-edge region and normalizing the post-edge to 1.0.

**Calculations.** All calculations in this work were performed with the electronic structure program ORCA.[28] Geometry optimizations were carried out using the BP86 functional.[29] A segmented all-electron relativistically contracted (SARC) basis set of triple-ζ-quality (TZVP) was used for rhenium and molybdenum with enhanced integration accuracy (SPECIALGRIDINTACC 14).[30] A scalar relativistic correction was applied using the zeroth-order regular approximation (ZORA) method.[31] An all-electron polarized triple-ζ-quality (TZVP) basis set of the Ahlrich's group was used for the other atoms.[32] Auxiliary basis sets for all complexes used to expand the electron density in the calculations were chosen to match the orbital basis. The self-consistent field (SCF) calculations were tightly converged ($1 \times 10^{-8}$ $E_h$ in energy, $1 \times 10^{-7}$ $E_h$ in the density change, and $1 \times 10^{-7}$ in the maximum element of the DIIS[33] error vector). The geometry search for all complexes was carried out in redundant internal coordinates without imposing geometry constraints. Canonical orbitals were constructed using the program Molekel.[34]

Time-dependent density functional theory (TD-DFT) calculations of the sulfur K-pre-edges using the BP86 functional were conducted as previously described.[20,21] Because of the limitations in the accurate treatment of excited states in DFT, absolute transition energies cannot be obtained by this method. Nevertheless, the relative transition energies and the relative intensities are, in general, reliably modeled. The six sulfur 1s orbitals were localized using the Pipek–Mezey criteria,[35] and the TD-DFT equations were solved[36] individually for each sulfur atom, excluding all but excitations originating from the sulfur 1s orbital.[10,12,20,21] It was established that constant shift of +61.45 eV is required for this regime of basis sets and applied to the transition energies to align calculated and experimental data. Plots were obtained using a variable line broadening of 0.75 to 1.2 eV.

## RESULTS AND DISCUSSION

**Syntheses and Crystallography.** Neutral $[Re(pdt)_3]$ (**2**) was prepared following the original recipe by Schrauzer and Mayweg of combining $ReCl_5$ with the thiophosphate ester obtained in situ from the reaction of benzoin and $P_4S_{10}$ in refluxing dioxane.[5,37] Chemical oxidation of **2** was achieved with "Magic Blue" (tris(4-bromophenyl)ammoniumyl hexachloroantimonate) stirring in $CH_2Cl_2$ to give dark green **1** in modest yields. Reduction of **2** with *n*-butyllithium gave chocolate brown **3** isolated as the tetraphenylphosphonium salt after addition of $PPh_4Br$ in methanol. Dark green **4** was prepared by the method devised by Connelly and McCleverty as the tetraphenylphosphonium salt.[9] With the exception of **3**, all complexes are dark green and readily soluble in chlorinated solvents and acetone; **3** is only appreciably soluble in DMF and DMA.

The crystal structures of **3**·DMF, **3**·DMA, and **4** have been determined by X-ray crystallography at 100(2) K. The structures of the anions in **3**·DMF and **4** are shown in Figure 1, and selected bond distances and angles are summarized in Table 2.

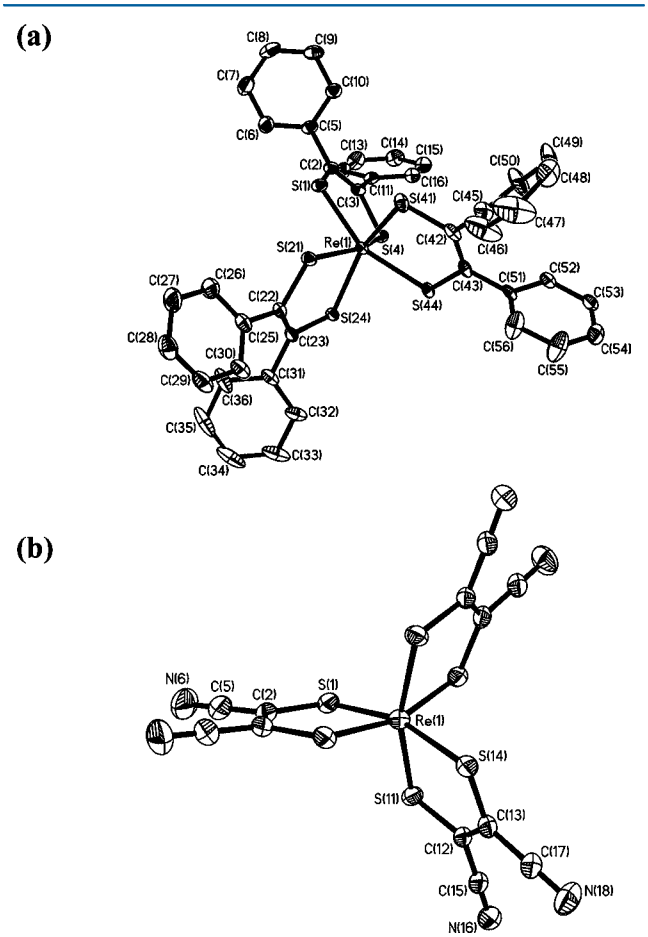


**Figure 1.** Structure of (a) the monoanion in crystals of **3**·DMF, and (b) the dianion in crystals of **4**.

The structure of **3**·DMF contains a monoanion, $[Re(pdt)_3]^-$, a well separated tetraphenylphosphonium cation, and one *N*,*N*′-dimethylformamide solvation molecule. The structure was


dx.doi.org/10.1021/ic2016534 | Inorg. Chem. 2011, 50, 12623–12631

**Table 2. Average Experimental and Calculated (DFT) Metric Parameters**

| | $[Re(pdt)_3]^{1+}$ | $[Re(pdt)_3]^0$ | | $[Re(pdt)_3]^{1-}$ | | $[Re(mnt)_3]^{2-}$ | |
|---|---|---|---|---|---|---|---|
| | calcd | exptl[a] | calcd | exptl | calcd | exptl | calcd |
| Re−S (Å) | 2.352 | 2.332(1) | 2.362 | 2.342(1) | 2.366 | 2.364(1) | 2.387 |
| S−C (Å) | 1.737 | 1.721(4) | 1.756 | 1.747(4) | 1.772 | 1.734(4) | 1.765 |
| C−C[b] (Å) | 1.397 | 1.374(5) | 1.378 | 1.349(5) | 1.371 | 1.359(6) | 1.389 |
| $S\cdots S_{inter}$ (Å)[c] | 3.071 | 3.055 | 3.106 | 3.148 | 3.189 | 3.210 | 3.271 |
| $SMS_{intra}$ (deg)[d] | 82.2 | 82.03(2) | 81.7 | 81.84(2) | 81.9 | 80.48(4) | 84.2 |
| $\alpha$ (deg)[e] | 0.2 | 1.3 | 0.3 | 4.4 | 0.5 | 3.0 | 4.9 |
| $\Theta$ (deg)[f] | 3.0 | 3.8 | 10.0 | 26.3 | 27.8 | 38.3 | 40.8 |

[a]Structure from ref 38. [b]Dithiolene carbon atoms. [c]Interligand S···S distance. [d]S−M−S intraligand bite angle. [e]Dithiolene fold angle, $\alpha$, defined as the dihedral angle between the $ReS_2$ and $S_2C_2$ planes of each bidentate ligand. [f]Trigonal or "Bailar" twist angle, $\Theta$, which is 0° in a trigonal prism and 60° in an octahedron.

highly disordered (Supporting Information, Figure S2a), and attempts to relieve the system by using a heavier solvent, in this case *N*,*N*′-dimethylacetamide, were unsuccessful (**3**·DMA, Supporting Information, Figures S1 and S2b). The $ReS_6$ polyhedron is distorted trigonal prismatic ($\Theta$ = 26.3°) unlike highly trigonal prismatic **2** ($\Theta$ = 3.8°).[38] Two other monoanionic complexes of this series, $[Re(tms)_3]^{1-}$ and $[Re(Cl_2\text{-bdt})_3]^{1-}$, crystallized with average twist angles of 0.5° and 24.8°, respectively, and this large variation attributed to the exceedingly flat potential energy surface for all monoanions with rhenium.[10] The average intraligand C−S (1.747 Å) and C−C (1.349 Å) bond lengths are consistent with C−S single bonds and C−C double bonds, respectively. These distances are longer and shorter, respectively, than the intraligand bonds in **2** that suggests this chemical reduction is predominantly ligand-centered, and that the electronic structure can be assigned as $[Re^{V}(L_3^{6-})]^{1-}$. The average Re−S bond length remains constant between **2** and **3**·DMF, supporting this formulation. Interestingly, the anion in **3**·DMF bears the same intraligand bond distances as for $[W(pdt)_3]^-$ whose electronic structure was more meaningfully described with resonance structures $\{[W^{IV}(L_3^{5-\bullet})]^{1-} \leftrightarrow [W^{V}(L_3^{6-})]^{1-}\}$.[11]

The crystal structure of **4** is the first example of structural characterization of a dianionic member of the tris(dithiolene)-rhenium series. As seen in all complexes with three $(mnt)^{2-}$ ligands,[11,12,39,40] the $ReS_6$ core approaches the octahedral limit at $\Theta$ = 38.3°.[41] It is clear from the structural parameters that $[Re(mnt)_3]^{2-}$ contains three closed-shell dithiolate ligands bound to a +IV central ion. The central Re(IV) ion is low-spin $d^3$ ($S = {}^1/_2$) and highlights the inherent preference for this configuration for second and third row transtions metals. As such, the Re(IV) ion exhibits a slight Jahn−Teller distortion with three shorter Re−S distances at ∼2.35 Å and three longer ones at ∼2.38 Å, which are faithfully reproduced by the DFT calculations (vide infra). Overall, based on the structural data for **2**− **4**, this electron transfer series is described as shown in Scheme 1. In the absence of a crystal structure, sulfur K-edge

**Scheme 1. Four-Membered Electron Transfer Series for $[Re(L_3)]^z$ ($z$ = 1+, 0, 1−, 2−)**

$$[Re^{V}(L_3^{4-})]^{1+} \underset{-e}{\overset{+e}{\rightleftharpoons}} [Re^{V}(L_3^{5-\bullet})]^{0} \underset{-e}{\overset{+e}{\rightleftharpoons}} [Re^{V}(L_3^{6-})]^{1-} \underset{-e}{\overset{+e}{\rightleftharpoons}} [Re^{IV}(L_3^{6-})]^{2-}$$

$S = 0$ $S = {}^1/_2$ $S = 0$ $S = {}^1/_2$

XAS data confirms the formulation for the monocation in **1** (vide infra) with trigonal prismatic ($D_{3h}$) molecular geometry.

**Sulfur K-Edge XAS.** An overlay of the normalized sulfur K-edge spectra for **1**−**4** and their second derivatives are shown in

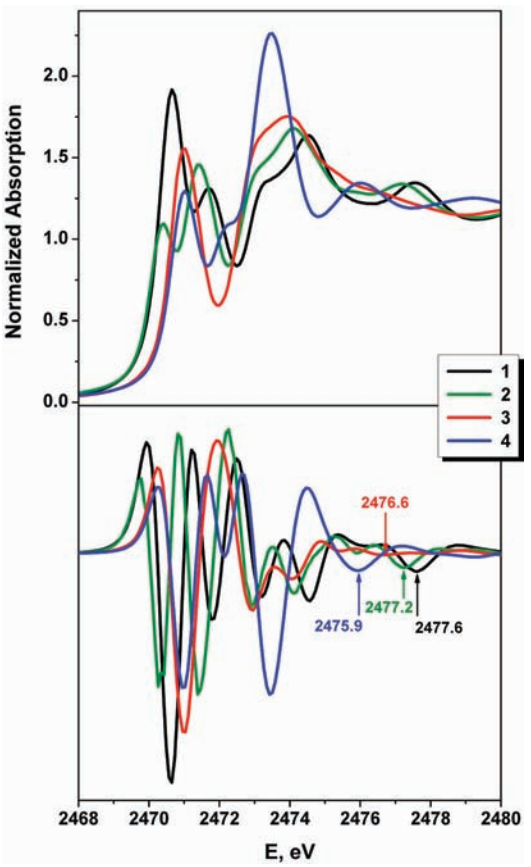


**Figure 2.** Comparison of the normalized S K-edge spectra (top) and their second derivatives (bottom) for complexes **1**−**4**. The arrows indicate the S 1s → 4p transition.

Figure 2. Individual pseudo-Voigt deconvolutions are displayed in Figure 3 with the pre-edge peak energies and intensities listed in Table 3.

There are two well resolved pre-edge features in the spectra of **1** and **2**, with the lowest energy peak occurring at 2470.65 and 2470.42 eV, respectively. This is 1 eV lower in energy than the second pre-edge peak at 2471.69 and 2471.42 eV for **1** and **2**, respectively. The low-energy transition is the fingerprint for a sulfur-centered radical,[10,12,21,39,42] in this case the S 1s → $2a_2'$ excitation where the acceptor orbital is distributed over the tris(dithiolene) ligand unit. The relative intensity of 2.15:1.00


dx.doi.org/10.1021/ic2016534 | Inorg. Chem. 2011, 50, 12623−12631

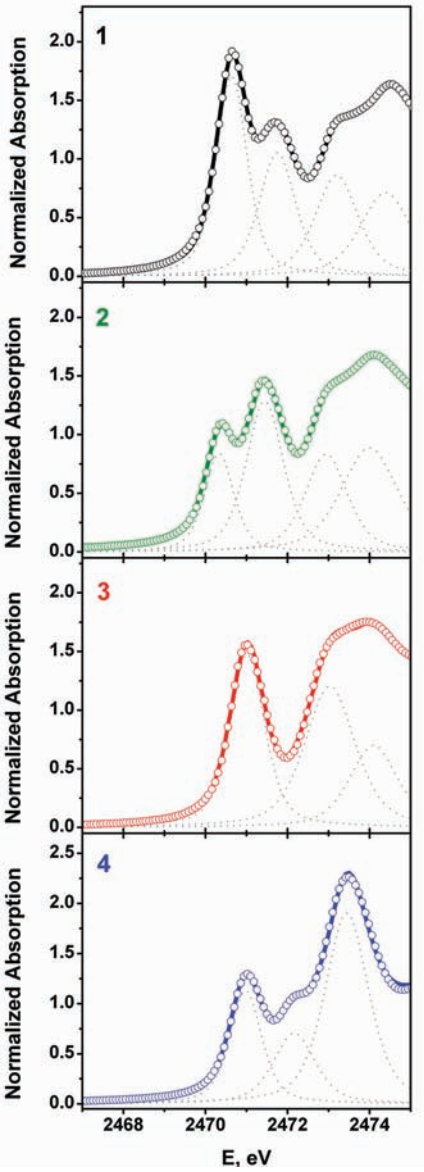


**Figure 3.** Pseudo-Voigt deconvolution of the S K-edge spectra of **1**–**4**. Circles represent the experimental data; dotted lines the pseudo-Voigt peaks; and the solid line the sum of the fit.

**Table 3. Pre-Edge Peak Energies ($E$), Intensities ($D_0$), Number of Holes in Acceptor Orbitals ($h$), and Covalencies (S 3p%) for the Tris(dithiolene)rhenium Series Studied**

| | $E$ (eV) | $D_0$ | $h$ | covalency[a] |
|---|---|---|---|---|
| **1** | 2470.65 | 1.53 | 2 | 87 |
| | 2471.69 | 1.11 | 4 | 32 |
| **2** | 2470.42 | 0.71 | 1 | 85 |
| | 2471.42 | 1.39 | 4 | 41 |
| **3** | 2471.03 | 1.48 | 4 | 47 |
| **4** | 2470.98 | 0.97 | 3 | 45 |

[a]Determined from $\alpha^2 = 18D_0/h \times I_s$ (see text). For **1**, $I_s = 15.78$; **2**, $I_s = 15.12$; **3**, $I_s = 14.10$; **4**, $I_s = 12.92$. Estimated from the S 1s → 4p transition energy in Figure 2 and the correlation plot in Figure 7 of ref 17.

here indicates that, as previously established, **2** contains an $(L_3)^{5-\bullet}$ unit (Scheme 1) with one oxidative hole, and for the first time, we have experimentally determined that **1** possesses an $(L_3)^{4-}$ unit with two oxidative holes in complete agreement with the computational prediction.[10] The anions in **3** and **4** exhibit one pre-edge peak at 2471.03 and 2470.98 eV, respectively, characterized as the S 1s → 5e′ ($d_{x^2-y^2,xy}$) transition. The absence of the lower energy feature identified in **1** and **2** clearly diagnoses the tris(dithiolene) unit as fully reduced, $(L_3)^{6-}$. For $[Re(pdt)_3]^{1+/0/1-}$, the progression to lower energy of this peak, 2471.69 to 2471.42 to 2471.03 eV upon reduction of **1** through **3**, demonstrates the ligand-centered nature of this reduction and therein retention of a Re(V) central ion. The variation in transition intensity is presumably a response to the structural rearrangement to $D_3$ symmetry. The decrease in intensity (34% based on area, Table 3) of the pre-edge peak in **4** compared to **3** is in keeping with reduction of the metal ion to Re(IV) with an electron added to the 5e′ level. The peaks beyond 2472 eV are transitions to C–S $\pi^*$ and C–S $\sigma^*$ orbitals frequently observed in the spectra of dithiolene[17,18,39,42,43] and thiolate[44] complexes, and are best assigned as "rising" edge features because they are followed by transitions to the sulfur 4p levels (vide infra) and finally into the continuum. The $mnt^{2-}$ ligands in **4** generate a lower energy rising-edge transition at 2472.14 eV (Figure 2) attributed to the S 1s → C–S $\pi^*$ transition with a significant contribution from the conjugated CN substituents.[17,39] The shift in the rising edge (comparing the peak at ~2474 eV in each spectrum) from **3** to **2** to **1** is further recognition of successive ligand oxidation.

**Calculations.** Spin-unrestricted Kohn–Sham (UKS) DFT calculations were carried out with inclusion of scalar relativistic effects using the ZORA method. In general, the calculated geometries and metrical parameters of the complexes in **1**–**4** presented in Table 2 were found to be in very good agreement with experimental values where available, and moreover, the trend in the Re–S and intraligand bond distances are representative of the metal and tris(dithiolene) oxidation levels. The twist angle, Θ, is well reproduced for the anions in **3** and **4**, and despite being calculated at 10.0° for **1**, significantly larger than the experimental value,[38] we have previously noted this represents only a very small difference in the total energy.[10] Most importantly, the monocation in **1** has no dithiolene fold ($\alpha = 0.2°$). This is significant because **1** is isoelectronic with neutral molybdenum and tungsten tris(dithiolenes) and monoanion vanadium tris(dithiolenes), which all display a pronounced distortion of this type.[11,12] For the first row metal, the lack of V–S covalency gives rise to a $(4e')^4(3a')^1(4a')^1(5e')^0$ electron configuration in $C_{3h}$ symmetry, where 3a′ is the metal-based ($d_{z^2}$) singly occupied molecular orbital (SOMO) and 4a′ is the ligand-based SOMO analogous to the $3a_1'$ and $2a_2'$ MOs in a $D_{3h}$ structure. Dithiolene folding occurs because it maximizes the antiferromagnetic coupling between the two unpaired electrons both in orbitals of a′ symmetry.[12] Isoelectronic neutral molybdenum and tungsten tris(dithiolenes) likewise fold, though here it is a second-order Jahn–Teller distortion that greatly stabilizes the metal-based highest occupied molecular orbital (HOMO) at the expense of the ligand-centered lowest unoccupied molecular orbital (LUMO) leading to an overall reduced total energy.[14,22] Being heavier metals, the antiferromagnetic coupling pathway is superseded by the high covalency in the M–S bonds, and therefore these bonds are not polarized. For **1**, the absence of a dithiolene fold clearly indicates that the $3a_1'$ (HOMO-1)–$2a_2'$ (LUMO) energy gap is too large for a second-order Jahn–Teller to be operative. In fact, the effective nuclear charge of Re stabilizes the $d_{z^2}$ ($3a_1'$) orbital relative to the highest occupied $\pi$


dx.doi.org/10.1021/ic2016534 | Inorg. Chem. 2011, 50, 12623–12631

bonding 4e′ MOs (Supporting Information, Figure S7). The LUMO remains the 100% ligand-based $2a_2'$ orbital.

Having previously detailed an in depth computational analysis of this electron transfer series,[10] the electronic configuration for this four-membered electron transfer series is as follows (with $D_{3h}$ symmetry labels): **1**, $(3a_1')^2(4e')^4(2a_2')^0(5e')^0$; **2**, $(3a_1')^2(4e')^4(2a_2')^1(5e')^0$; **3**, $(3a_1')^2(4e')^4(2a_2')^2(5e')^0$; **4**, $(4e')^4(3a_1')^2(2a_2')^2(5e')^1$. A qualitative depiction of the frontier orbitals across the series is presented in Supporting Information, Figure S7 identifying the electronic structures as $[Re^V(L_3^{4-})]^{1+}$ ($S = 0$), $[Re^V(L_3^{5-\bullet})]^0$ ($S = {}^1/_2$), $[Re^V(L_3^{6-})]^{1-}$ ($S = 0$), and $[Re^{IV}(L_3^{6-})]^{2-}$ ($S = {}^1/_2$), as shown in Scheme 1.

**Experimental Covalency.** Sulfur K-edge XAS has been successfully utilized to directly probe metal−ligand bonding in coordination complexes and enzymes.[15] In this context, covalency is defined as the ligand contribution to bonding, which is experimentally determined from the intensity ($D_0$) of the S 1s → 3p excitations to acceptor orbitals with some sulfur character, given by

$$D_0(\mathrm{S\ 1s} \rightarrow \Psi^*) = \alpha^2 h I_s / 3n$$

where $\alpha^2$ is the amount of sulfur 3p content (i.e., covalency), $h$ is the number of holes in the acceptor orbitals, $I_s$ is the radial transition dipole integral of the electric dipole allowed S 1s → 3p transition, $|\langle S_{1s}|r|S_{3p}\rangle|^2$, and $n$ is the number of absorbing sulfur atoms.[17,18,22] It has been shown through a combination of experiment and theory that the transition dipole integral, $I_s$ varies linearly (with a 3% quadratic component) with the energy of the S 1s → 4p transition, and the $I_s$ values for a variety of S-donor ligands have been estimated by this method.[17] From these experimental values, the covalencies were extracted from the peak areas.

For the current series of compounds, the S 1s → 4p transition is shown in the second derivative in Figure 2 as estimated from DFT calculations, and in part from the plausibility of the energy. The $I_s$ value for the $[Mo(mdt)_3]^{0/1-/2-}$ compounds was estimated at 14.22 based on an experimental S 1s → 4p peak at ∼2476.7 eV visible in the second derivative of all three spectra.[22] The absence of variation in this peak was ascribed to the contributions from all three ligands that average out the changes of ligand oxidation state. Moreover, it is the only peak seen at an energy expected for the S 1s → 4p transition. For $[Re(pdt)_3]^{1+/0/1-}$, there is a decrease in the S 1s → 4p transition concomitant with successive reduction of the tris(dithiolene) unit across this series from monocation (2477.6 eV) to neutral (2477.2 eV) to monoanion (2476.6 eV). Also, there is an additional destabilization of the 4p orbitals from the larger interligand repulsion in trigonal prismatic **1** and **2**. These energies are slightly higher than for the $[Mo(mdt)_3]^z$ ($z = 0, 1-, 2-$) series which is attributed to the subtle difference between electron donating methyl and electron withdrawing phenyl substituents. Using the calibration plot developed by Solomon and co-workers,[17] the $I_s$ values for the S 1s → 3p transition in **1**, **2**, and **3** work out as 15.78, 15.12, and 14.10, respectively. The S 1s → 4p transition in **4** is located at 2475.9 eV, much lower than the pdt-containing complexes. A value of 2476.6 eV was identified in $[Cu(mnt)_2]^{2-}$,[17] with the shift to higher energy plausibly ascribed to greater interligand repulsion in the square planar complex;[45] the average S···S distance is 3.005 Å compared with 3.210 Å in **4** (Table 2). The computed $I_s$ for **4** is then 12.92.

Using these $I_s$ values, the experimental covalencies for the two pre-edge transitions in **1** and **2**, and one in **3** and **4** have been estimated (Table 3). The intensities ($D_0$) are derived from pseudo-Voigt deconvolution of the pre-edge peaks (Figure 3). For the S 1s → $2a_2'$ excitation, the estimated S 3p content is clearly too high (>80%), a marked overestimation compared to previous experimental and calculated composition of this dithiolene $\pi$ orbital.[10−12,18,22,39,46] The values obtained for the S 3p contribution to the 5e′ level are more reasonable, and match those computed for the corresponding $[Re(bdt)_3]^z$ ($z = 1+, 0, 1-, 2-, 3-$) series.[10]

**Time-Dependent DFT Calculations.** The difficulty in identifying an obscure transition beyond the edge presents a challenge in accurately determining the experimental covalency from the transition dipole integral (vide supra). Therefore, a simple TD-DFT approach has been successfully deployed as an alternative means at defining metal−sulfur covalency in transition metal dithiolene complexes.[10,12,19,21,39,40] This approach involves calculating the oscillator strength of the S 1s → 3p transition since neither $I_s$ nor $\alpha^2$ are experimentally observable. The results from TD-DFT calculations of the S K-pre-edge spectra of **1**−**4** at the BP86 level of theory are presented in Table 4. The data were computed on the optimized coordinates rather than the crystallographic ones with negligible difference in their computed spectral profile (Supporting Information, Figure S8) and orbital composition (Supporting Information, Table S7).

**Table 4. Comparison of Experimental and Calculated Pre-Edge Peak Energies ($E$), Intensities ($D_0$) and Oscillator Strengths ($f_{osc}$) for Complexes 1−4**

| | $E$ (eV) | | $D_0$[b] | $f_{osc}$ (×10³) | |
|---|---|---|---|---|---|
| | exptl | calcd[a] | | exptl[c] | calcd[d] |
| **1** | 2470.65 | 2470.63 | 1.53 | 6.14 | 5.22 |
| | 2471.69 | 2471.71 | 1.11 | 6.56 | 8.22 |
| **2** | 2470.42 | 2470.38 | 0.71 | 2.85 | 2.85 |
| | 2471.42 | 2471.45 | 1.39 | 7.84 | 7.84 |
| **3** | 2471.03 | 2471.02 | 1.48 | 8.35 | 7.36 |
| **4** | 2470.98 | 2470.84 | 0.97 | 5.47 | 4.83 |

[a]Energy shifted +61.45 eV. [b]Intensities derived from area of fitted pseudo-Voigt peak from Figure 3. [c]$[Re(pdt)_3]$ calibrated data. [d]Dipolar oscillator strengths.

The calculated spectra are contrasted with the experimental data in Figure 4 and show excellent agreement in regard to the calculated peak energies (Table 4). Neutral **2** was chosen as the standard because it possesses both pre-edge transitions and, unlike **1**, has been structurally characterized.[1,38] The computed pre-edge transition energies for **2** nicely match the experimental data (after empirical correction) though there is a noticeable difference in intensity ratio between the first two pre-edge peaks (1.0:2.0 experimental; 1.0:2.7 calculated). The calculated oscillator strengths of 2.85 and 7.85 for the S 1s → $2a_2'$ and S 1s → 5e′ transitions in **2**, respectively, account for peak areas of 0.71 and 1.39 units.[2] Using these fixed values for the respective pre-edge transitions, the experimental oscillator strengths were computed and compared to the values derived from TD-DFT (Table 4). Overall, there is very good agreement between experiment and theory. The experimental trend of increasing oscillator strength in the S 1s → 5e′ transition from **1**− **3** is reversed in the calculations which must arise from an


dx.doi.org/10.1021/ic2016534 | Inorg. Chem. 2011, 50, 12623−12631

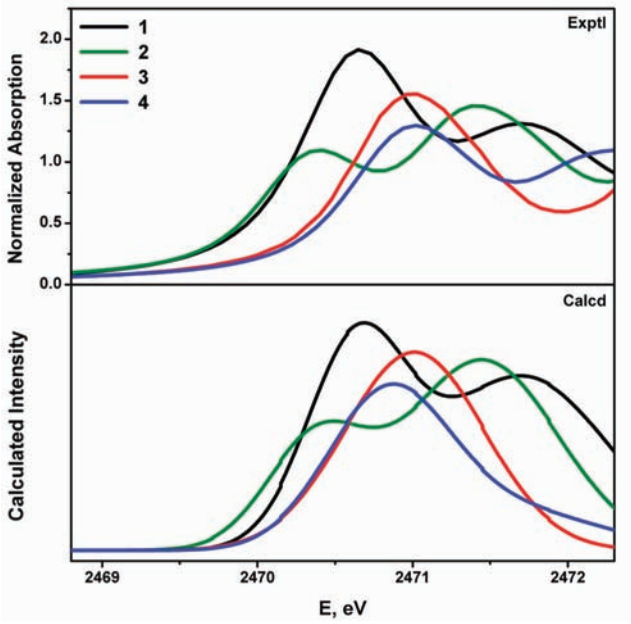


**Figure 4.** Comparison of the experimental (top) and calculated (bottom) S K-pre-edge spectra for complexes **1**–**4** obtained from ZORA-BP86 TD-DFT calculations. Calculated intensity in arbitrary units.

underestimation in **1** and overestimation in **3** of the sulfur contribution to the 5e′ orbitals.

The two methods of estimating the covalency—the $I_s$ computed and $[Re(pdt)_3]$ calibrated—are contrasted in Table 5 along with the S 3p content calculated by DFT. Certainly the best agreement comes from the $[Re(pdt)_3]$ calibrated data, perhaps because of an inherent assumption used in determining $I_s$, that the charge on the S atoms is the dominant contributor to the radical transition dipole integral. It is known, and has been reported in an analogous study of transition metal bis(dithiolene) complexes,[21] that the radial distortion of the acceptor orbitals depends on the degree of overlap between the constituent atomic orbitals (or fragments). It was shown that $I_s$ values are expected for a transition to an acceptor orbital that is $\sigma$ bonding than one that is $\pi$ bonding. Orbitals involved in $\pi$ bonding are more contracted than their $\sigma$ counterparts, and as such, their $\pi^*$ equivalents are less antibonding than the $\sigma^*$ bonds, and therein have smaller $I_s$ values. This undermines the assumption that all S 1s → 3p transitions are the same, exposing an intrinsic flaw in the covalency estimation. It is apparent from the comparison in Table 5 that the antibonding nature of the $2a_2'$ and 5e′ MOs are quite different, with the covalency overestimated by a staggering 70% for the $2a_2'$ MO in **1**. This is the first time an excitation to a nonbonding acceptor orbital has been analyzed, and surprisingly the $2a_2'$ MO appears to have more antibonding character than the $\pi^*$ 5e′ MOs, and hence the stark disagreement between experiment and theory. The agreement between experiment and theory for the 5e′ composition is marginally better for the $[Re(pdt)_3]$ calibrated data.

We have examined two related complexes bearing the same dithiolene ligand, $[V(pdt)_3]^{0/1-}$. Their electronic structure has previously been spectroscopically and computationally assigned as $[V^{IV}(L_3^{4-})]^0$ and $[V^{IV}(L_3^{5-\bullet})]^{1-}$, respectively, and both exhibit two pre-edge peaks in their S K-edge spectra concomitant with oxidized ligands (Supporting Information, Figure S9).[12] Using the calibrated oscillator strengths, there is very good agreement in the estimated covalency as opposed to the $I_s$ derived values. Moreover, the data also reflect the large polarization of the V–S bonds in this series, with the second pre-edge peak corresponding to excitations to the 5e′($\alpha$) orbitals only. For $[V^{IV}(pdt)_3]$, the addition of the 1s → 3a′($\beta$) to this second pre-edge feature brings the total intensity to 32.3% in excellent agreement with the experimental estimate of 31.7%.

**Table 5. Calculated and Experimental Covalencies for the Tris(dithiolene) Complexes**

| | | | | experimental covalency[a] | | |
|---|---|---|---|---|---|---|
| | complex symmetry | transition | $h$ | $A$ | $B$ | calculated covalency[b] |
| $[Re^{V}(pdt)_3]^{1+}$ | $D_{3h}$ | 1s → $2a_2'$ | 2 | 87.3 | 62.8 | 51.5 |
| | | 1s → 5e′ | 4 | 31.7 | 32.1 | 40.5 |
| $[Re^{V}(pdt)_3]^{0}$ | $D_{3h}$ | 1s → $2a_2'(\beta)$ | 1 | 84.5 | 58.3 | 58.3 |
| | | 1s → 5e′ | 4 | 41.4 | 40.2 | 40.2 |
| $[Re^{V}(pdt)_3]^{1-}$ | $D_3$ | 1s → 5e | 4 | 47.2 | 42.7 | 39.4 |
| $[Re^{IV}(mnt)_3]^{2-}$ | $D_3$ | 1s → 5e | 3 | 45.0 | 37.4 | 33.8 |
| $[V^{IV}(pdt)_3]^{0}$ [c] | $D_{3h}$ | 1s → $2a_2'$ | 2 | 78.6 | 52.2 | 62.1 |
| | | 1s → 3a′($\beta$) | 1 | | | 4.1 |
| | | 1s → 5e′($\alpha$) | 2 | 33.9 | 31.7 | 28.2 |
| $[V^{IV}(pdt)_3]^{1-}$ [c] | $C_{3h}$ | 1s → 4a′($\alpha$) | 1 | 117.4 | 72.0 | 64.0 |
| | | 1s → 3a′($\beta$) | 1 | | | 9.7 |
| | | 1s → 5e′($\alpha$) | 2 | 35.3 | 30.5 | 29.9 |
| $[Mo^{IV}(mdt)_3]^{0}$ [d] | $C_{3h}$ | 1s → 4a′ | 2 | 69 | 44.8 | 52.5 |
| | | 1s → 5e′ | 4 | 27 | 24.6 | 36.9 |
| $[Mo^{IV}(mdt)_3]^{1-}$ [d] | $D_{3h}$ | 1s → $2a_2'(\beta)$ | 1 | 75 | 48.4 | 68.9 |
| | | 1s → 5e′ | 4 | 37 | 33.5 | 34.3 |
| $[Mo^{IV}(mdt)_3]^{2-}$ [d] | $D_{3h}$ | 1s → 5e′ | 4 | 36 | 32.6 | 32.5 |

[a]Presented as S 3p% per hole, $h$. Method A: covalency from experimental $I_s$ value. Method B: $[Re(pdt)_3]$ calibrated experimental covalency. [b]Derived from ZORA-BP86 DFT calculations. [c]Derived from B3LYP DFT calculations described in ref 12. $[V(pdt)_3]$: $I_s$ = 14.57; $[V(pdt)_3]^{1-}$: $I_s$ = 13.45. [d]Experimental covalencies by Method A taken from ref 22. Calculated covalency derived from ZORA-BP86 DFT single point calculation with crystallographic coordinates.


dx.doi.org/10.1021/ic2016534 | Inorg. Chem. 2011, 50, 12623–12631

Given the similarity of $pdt_3$ and $mdt_3$ tris(dithiolene) units, we investigated the experimental covalency for the $[Mo(mdt)_3]^z$ ($z$ = 0, 1−, 2−) series and contrasted it with values derived from the $I_s$ estimate.[22] It was noted recently that the intensity of the first-edge peak in $[Mo(mdt)_3]$ is considerably less intense than for $[Re(pdt)_3]^{1+}$,[47] which is difficult to fathom since both have been characterized with an $(L_3)^{4-}$ ligand set encapsulating a $d^2$ metal ion. The results of the analysis are presented in Table 5 along with a comparison of the DFT derived values from single point calculations on the crystal structure coordinates.[48,49] It should be noted that there is very little difference between our calculated values posted here and those performed by Solomon and co-workers.[22] The results show almost no difference between the two methods for the covalency in the 5e′ MOs, which nicely match the theory. For $[Mo(mdt)_3]$ there is a significant difference between all three values, with the $[Re(pdt)_3]$ calibrated value being closer to the theoretical one. However, the opposite is seen for $[Mo(mdt)_3]^{1-}$, which is not so readily understood. As noted above, neutral molybdenum and tungsten tris(dithiolene) complexes exhibit a geometric distortion (dithiolene fold) that represents a lowering of symmetry $D_{3h} \rightarrow C_{3h}$, mixing the HOMO and LUMO. The requirement for this distortion is a small HOMO−LUMO energy gap,[50] and that the mixing of these two orbitals stabilizes the HOMO and lowers the total energy of the molecule. For isoelectronic $[Re^V(L_3^{4-})]^{1+}$, only a $D_{3h}$ symmetric geometry was ever observed in geometry optimizations (vide supra) indicating a much larger energy gap between the $3a_1'$ HOMO-1 and $2a_2'$ LUMO which is not unexpected for this heavier metal (Supporting Information, Figure S7). Therefore, the first pre-edge transition is to the nonbonding $2a_2'$ orbital, whereas it is to the 4a′ MO in $[Mo(mdt)_3]$ that is no longer exclusively ligand-based. The distortion introduces d character into the LUMO, and ligand character into the now stabilized HOMO (Supporting Information, Table S8), such that the electronic structure is best represented as resonance structures $\{[Mo^{IV}(L_3^{4-})]^0 \leftrightarrow [Mo^V(L_3^{5-\bullet})]^0\}$. The magnitude of the fold governs the contributions from the two resonance forms, so with a fold of 16° in $[Mo(mdt)_3]$,[49] compared with 23.8° in $[Mo(tbbdt)_3]$ ($tbbdt^{2-}$ = 3,5-di-*tert*-butylbenzene-1,2-dithiolate)[42] the former is closer to the $[Mo^{IV}(L_3^{4-})]^0$ formulation while the latter has greater contribution from the Mo(V) form. In the isoelectronic vanadium tris(dithiolene) monoanions, the highly polarizable V−S bonds ensue a $[V^{IV}(L_3^{5-\bullet})]^{1-}$ formulation, where strong antiferromagnetic coupling between metal and ligand radicals drives the distortion rather than HOMO−LUMO mixing.[12]

## CONCLUSIONS

Unlike previous transition metal tris(dithiolene) electron transfer series, the $[Re(L_3)]^z$ ($z$ = 1+, 0, 1−, 2−) series studied here is conveniently transcended by only one geometric distortion: a twist about the 3-fold axis. This comes about from the large effective nuclear charge and relativistic potential of the Re ion which greatly stabilizes its d shell. Therefore, this series is the perfect calibrant for S K-edge XAS determination of metal−ligand covalency in tris(dithiolene) complexes. Using the well characterized $[Re(pdt)_3]$ (**2**) as a standard, the intensity of the pre-edge transitions to the nonbonding $2a_2'$ MO and the $\pi^*$ 5e′ MOs, that have one and four holes, respectively, the covalency of the other three-members of this series are experimentally quantified. For the first time, a rhenium tris(dithiolene) monocation has been isolated and spectroscopically characterized, and the proposed molecular and electronic structure[10] verified by its S K-edge spectrum. The first pre-edge peak in **1** is double that of **2** consistent with ligand-centered oxidation and formulated as $[Re^V(L_3^{4-})]^{1+}$. The loss of this peak in **3** and **4** identifies a fully reduced tris(dithiolene) unit in each (Scheme 1).

Using these benchmarks, the covalency in the analogous vanadium and molybdenum tris(dithiolene) series are more accurately estimated with the TD-DFT approach than using the radial dipole integral. The assignment of oxidation levels in neutral tris(dithiolene)molybdenum compounds—isoelectronic to the monocation in **1**—has been refined, in that the dithiolene fold which mixes the HOMO and LUMO leads to an electronic structure best defined by the resonance forms $\{[Mo^{IV}(L_3^{4-})]^0 \leftrightarrow [Mo^V(L_3^{5-\bullet})]^0\}$. The magnitude of the fold angle modulates the d character, and therefore, akin to monoanionic cobalt bis(dithiolene) complexes,[51] the metal has a noninteger oxidation state. The same definition is applied to analogous tungsten complexes but not isolectronic tris(dithiolene)vanadium monoanions, where dithiolene folding strengthens the antiferromagnetic coupling between metal- and ligand-based unpaired electrons. Given the limited number of available transition metal tris(dithiolene) compounds and moreover their lack of structural homogeneity, unlike their persistently square planar bis(dithiolene) counterparts, factors contributing to their observed trigonal prismatic geometry may never be fully revealed. Nevertheless, sulfur K-edge XAS remains the most effective spectroscopic technique to locate valence electrons in tris(dithiolene) complexes, and leads to clear description of the electron structures of any electron transfer series of this type.

## ASSOCIATED CONTENT

### Supporting Information

X-ray crystallographic files in CIF format for **3**·DMF, **3**·DMA, and **4**. S K-edge XAS spectra and their second derivatives for $[V(pdt)_3]^{0/1-}$. Tabulated metric parameters, optimized coordinates, and compositions of selected MOs for **1**−**4**, $[V(pdt)_3]^{0/1-}$, and $[Mo(mdt)_3]^{0/1-/2-}$. This material is available free of charge via the Internet at http://pubs.acs.org.

## AUTHOR INFORMATION

### Corresponding Author

*E-mail: sproules@mpi-muelheim.mpg.de.

## ACKNOWLEDGMENTS

We are grateful to the ANKA Synchrotron Light Source, Karlsruhe, Germany, for provision of beam time at the SCD beamline and Dr. Gernot Buth for assistance. We thank Prof. Serena DeBeer for assistance with XAS data collection. S.S. thanks the Max-Planck-Society for a postdoctoral fellowship. SSRL operations are funded by the Department of Energy, Office of Basic Energy Sciences. The Structural Molecular Biology program is supported by the National Institutes of Health (Grant 5 P41 RR001209), National Center for Research Resources, Biomedical Technology Program and by the Department of Energy, Office of Biological Environmental Research.

## REFERENCES

(1) (a) Eisenberg, R.; Ibers, J. A. *J. Am. Chem. Soc.* **1965**, *87*, 3776. (b) Eisenberg, R.; Ibers, J. A. *Inorg. Chem.* **1966**, *5*, 411.
(2) Stiefel, E. I.; Brown, G. F. *Inorg. Chem.* **1972**, *11*, 434.

(3) Eisenberg, R. *Coord. Chem. Rev.* **2011**, *255*, 825.
(4) (a) Al-Mowali, A. H.; Porte, A. L. *J. Chem. Soc., Dalton Trans.* **1975**, 50. (b) Eisenberg, R.; Stiefel, E. I.; Rosenberg, R. C.; Gray, H. B. *J. Am. Chem. Soc.* **1966**, *88*, 2874. (c) Stiefel, E. I.; Dori, Z.; Gray, H. B. *J. Am. Chem. Soc.* **1967**, *89*, 3353.
(5) Schrauzer, G. N.; Mayweg, V. P. *J. Am. Chem. Soc.* **1966**, *88*, 3235.
(6) Stiefel, E. I.; Eisenberg, R.; Rosenberg, R. C.; Gray, H. B. *J. Am. Chem. Soc.* **1966**, *88*, 2956.
(7) Wharton, E. J.; McCleverty, J. A. *J. Chem. Soc. A* **1969**, 2258.
(8) (a) Best, S. P.; Ciniawsky, S. A.; Humphrey, D. G. *J. Chem. Soc., Dalton Trans.* **1996**, 2945. (b) Best, S. P.; Clark, R. J. H.; McQueen, R. C. S.; Walton, J. R. *Inorg. Chem.* **1988**, *27*, 884. (c) Stiefel, E. I.; Bennett, L. E.; Dori, Z.; Crawford, T. H.; Simo, C.; Gray, H. B. *Inorg. Chem.* **1970**, *9*, 281.
(9) Connelly, N. G.; Jones, C. J.; McCleverty, J. A. *J. Chem. Soc. A* **1971**, 712.
(10) Sproules, S.; Benedito, F. L.; Bill, E.; Weyhermüller, T.; DeBeer George, S.; Wieghardt, K. *Inorg. Chem.* **2009**, *48*, 10926.
(11) Sproules, S.; Banerjee, P.; Weyhermüller, T.; Yan, Y.; Donahue, J. P.; Wieghardt, K. *Inorg. Chem.* **2011**, *50*, 7106.
(12) Sproules, S.; Weyhermüller, T.; DeBeer, S.; Wieghardt, K. *Inorg. Chem.* **2010**, *49*, 5241.
(13) (a) Cowie, M.; Bennett, M. J. *Inorg. Chem.* **1976**, *15*, 1584. (b) Smith, A. E.; Schrauzer, G. N.; Mayweg, V. P.; Heinrich, W. *J. Am. Chem. Soc.* **1965**, *87*, 5798.
(14) Campbell, S.; Harris, S. *Inorg. Chem.* **1996**, *35*, 3285.
(15) (a) Glaser, T.; Hedman, B.; Hodgson, K. O.; Solomon, E. I. *Acc. Chem. Res.* **2000**, *33*, 859. (b) Solomon, E. I.; Hedman, B.; Hodgson, K. O.; Dey, A.; Szilagyi, R. K. *Coord. Chem. Rev.* **2005**, *249*, 97.
(16) Neese, F.; Hedman, B.; Hodgson, K. O.; Solomon, E. I. *Inorg. Chem.* **1999**, *38*, 4854.
(17) Sarangi, R.; DeBeer George, S.; Jackson Rudd, D.; Szilagyi, R. K.; Ribas, X.; Rovira, C.; Almeida, M.; Hodgson, K. O.; Hedman, B.; Solomon, E. I. *J. Am. Chem. Soc.* **2007**, *129*, 2316.
(18) Szilagyi, R. K.; Lim, B. S.; Glaser, T.; Holm, R. H.; Hedman, B.; Hodgson, K. O.; Solomon, E. I. *J. Am. Chem. Soc.* **2003**, *125*, 9158.
(19) DeBeer George, S.; Neese, F. *Inorg. Chem.* **2010**, *49*, 1849.
(20) DeBeer George, S.; Petrenko, T.; Neese, F. *Inorg. Chim. Acta* **2008**, *361*, 965.
(21) Ray, K.; DeBeer George, S.; Solomon, E. I.; Wieghardt, K.; Neese, F. *Chem.—Eur. J.* **2007**, *13*, 2783.
(22) Tenderholt, A. L.; Szilagyi, R. K.; Holm, R. H.; Hodgson, K. O.; Hedman, B.; Solomon, E. I. *Inorg. Chem.* **2008**, *47*, 6382.
(23) *SAINT v7.46A*; Bruker AXS Inc.: Madison, WI, 2003.
(24) Sheldrick, G. M. *SADABS*, Bruker-Siemens Area Detector Absorption and Other Corrections, Version 2006/1; Universität Göttingen: Göttingen, Germany, 2006.
(25) *ShelXTL 6.14*; Bruker AXS Inc.: Madison, WI, 2003.
(26) Sheldrick, G. M. *ShelXL97*; Universität Göttingen: Göttingen, Germany, 1997.
(27) Hedman, B.; Frank, P.; Gheller, S. F.; Roe, A. L.; Newton, W. E.; Hodgson, K. O. *J. Am. Chem. Soc.* **1988**, *110*, 3798.
(28) Neese, F. *Orca, an Ab Initio, Density Functional and Semiempirical Electronic Structure Program Package*, version 2.8; Universität Bonn: Bonn, Germany, 2010.
(29) (a) Becke, A. D. *J. Chem. Phys.* **1993**, *98*, 5648. (b) Lee, C. T.; Yang, W. T.; Parr, R. G. *Phys. Rev. B* **1988**, *37*, 785.
(30) Pantazis, D. A.; Chen, X.-Y.; Landis, C. R.; Neese, F. *J. Chem. Theory Comput.* **2008**, *4*, 908.
(31) (a) van Lenthe, E.; Snijders, J. G.; Baerends, E. J. *J. Chem. Phys.* **1996**, *105*, 6505. (b) van Lenthe, J. H.; Faas, S.; Snijders, J. G. *Chem. Phys. Lett.* **2000**, *328*, 107. (c) van Lenthe, E.; van der Avoird, A.; Wormer, P. E. S. *J. Chem. Phys.* **1998**, *108*, 4783.
(32) (a) Ahlrichs, R.; May, K. *Phys. Chem. Chem. Phys.* **2000**, *2*, 943. (b) Schäfer, A.; Horn, H.; Ahlrichs, R. *J. Chem. Phys.* **1992**, *97*, 2571. (c) Schäfer, A.; Huber, C.; Ahlrichs, R. *J. Chem. Phys.* **1994**, *100*, 5829.
(33) (a) Pulay, P. *Chem. Phys. Lett.* **1980**, *73*, 393. (b) Pulay, P. *J. Comput. Chem.* **1982**, *3*, 556.
(34) *Molekel*, Advanced Interactive 3D-Graphics for Molecular Sciences; Swiss National Supercomputing Center: Manno, Switzerland; http://www.cscs.ch/molkel.
(35) Pipek, J.; Mezey, P. G. *J. Chem. Phys.* **1989**, *90*, 4916.
(36) Neese, F.; Olbrich, G. *Chem. Phys. Lett.* **2002**, *362*, 170.
(37) Schrauzer, G. N.; Finck, H. W.; Mayweg, V. P. *Angew. Chem.* **1964**, *76*, 715.
(38) Eisenberg, R.; Brennessel, W. W. *Acta Crystallogr.* **2006**, *C62*, m464.
(39) Banerjee, P.; Sproules, S.; Weyhermüller, T.; DeBeer George, S.; Wieghardt, K. *Inorg. Chem.* **2009**, *48*, 5829.
(40) Milsmann, C.; Sproules, S.; Bill, E.; Weyhermüller, T.; DeBeer George, S.; Wieghardt, K. *Chem.—Eur. J.* **2010**, *16*, 3628.
(41) The magnitude of the twist angle Θ is a function of the bite angle of a bidentate ligand. The normalized bite angle is defined as the distance between the donor atoms of the chelate divided by the metal−ligand bond length (Kepert, D. L. *Prog. Inorg. Chem.* **1977**, *23*, 1). From this value, an octahedral limit ($\Theta_{lim}$) can be determined for any given complex.
(42) Kapre, R. R.; Bothe, E.; Weyhermüller, T.; DeBeer George, S.; Wieghardt, K. *Inorg. Chem.* **2007**, *46*, 5642.
(43) Kapre, R. R.; Bothe, E.; Weyhermüller, T.; DeBeer George, S.; Muresan, N.; Wieghardt, K. *Inorg. Chem.* **2007**, *46*, 7827.
(44) (a) Dey, A.; Glaser, T.; Couture, M. M.-J.; Eltis, L. D.; Holm, R. H.; Hedman, B.; Hodgson, K. O.; Solomon, E. I. *J. Am. Chem. Soc.* **2004**, *126*, 8320. (b) Glaser, T.; Rose, K.; Shadle, S. E.; Hedman, B.; Hodgson, K. O.; Solomon, E. I. *J. Am. Chem. Soc.* **2001**, *123*, 442.
(45) Plumlee, K. W.; Hoffman, B. M.; Ibers, J. A.; Soos, Z. G. *J. Chem. Phys.* **1975**, *63*, 1926.
(46) (a) Ray, K.; Weyhermüller, T.; Neese, F.; Wieghardt, K. *Inorg. Chem.* **2005**, *44*, 5345. (b) Huyett, J. E.; Choudhury, S. B.; Eichhorn, D. M.; Bryngelson, P. A.; Maroney, M. J.; Hoffman, B. M. *Inorg. Chem.* **1998**, *37*, 1361. (c) Lim, B. S.; Fomitchev, D.; Holm, R. H. *Inorg. Chem.* **2001**, *40*, 4257.
(47) Sproules, S.; Wieghardt, K. *Coord. Chem. Rev.* **2011**, *255*, 837.
(48) Fomitchev, D.; Lim, B. S.; Holm, R. H. *Inorg. Chem.* **2001**, *40*, 645.
(49) Lim, B. S.; Donahue, J.; Holm, R. H. *Inorg. Chem.* **2000**, *39*, 263.
(50) Albright, T. A.; Burdett, J. K.; Whangbo, M. H. *Orbital Interactions in Chemistry, 1*; John Wiley and Sons, Inc.: New York, 1985.
(51) Ray, K.; Begum, A.; Weyhermüller, T.; Piligkos, S.; van Slageren, J.; Neese, F.; Wieghardt, K. *J. Am. Chem. Soc.* **2005**, *127*, 4403.